

## Comparison of the diffusion approximation and the discrete ordinates method for the investigation of heat transfer in glass

Kong Hoon Lee<sup>1)</sup> and Raymond Viskanta

School of Mechanical Engineering, Purdue University, West Lafayette, IN (USA)

---

Heat transfer by combined conduction and radiation has been investigated in a one-dimensional glass layer. The layer is semitransparent to radiation and the dependence of the absorption coefficient on wavelength is accounted for. The discrete ordinates method and the diffusion approximation are used to analyze radiative transfer. The differencing scheme for the discrete ordinates method has been investigated to obtain the constant total heat flux distribution across the glass layer as required by the energy conservation equation, and the best uniformity is obtained with the diamond scheme. The results predicted by the discrete ordinates method are in good agreement with those based on the exact (integral) equation formulation of radiative transfer. The diffusion approximation greatly underpredicts the temperature and heat flux distributions in the glass layer when the thickness or the opacity of the layer is small. The predictions of the diffusion approximation are only reasonable for thick glass layers. This approximation should be used with extreme caution to obtain quantitatively accurate results.

### Vergleich des Diffusionsansatzes und der Methode der diskreten Ordinaten zur Untersuchung des Wärmetransports in Glas

Die Wärmeübertragung durch Leitung und Strahlung wird in einer eindimensionalen Glasschicht untersucht. Die Schicht ist semitransparent gegenüber der Wärmestrahlung, die Abhängigkeit des Absorptionskoeffizienten von der Wellenlänge ist bekannt. Die Methode der diskreten Ordinaten und der Diffusionsansatz werden angewandt, um die Wärmeübertragung durch Strahlung zu analysieren. Das Differenzenschema für die Methode der diskreten Ordinaten wurde untersucht, um die konstante gesamte Verteilung des Wärmeflusses über die Glasschicht zu erhalten, wie es die Energieerhaltungsgleichung verlangt. Die beste Übereinstimmung wird mit dem „diamond“-Schema erreicht. Die nach der Methode der diskreten Ordinaten vorausgesagten Ergebnisse stimmen gut mit denjenigen überein, die mit der exakten (integralen) Gleichung der Wärmeübertragung durch Strahlung erhalten werden. Der Diffusionsansatz unterdrückt die Temperatur- und die Wärmeflußverteilung in der Glasschicht zu stark, wenn die Dicke oder die Lichtundurchlässigkeit der Schicht klein ist. Die Voraussagen dieses Ansatzes sind nur für dicke Glasschichten aussagekräftig; er sollte mit großer Vorsicht angewendet werden, damit man quantitativ richtige Resultate erhält.

### 1. Introduction

In the manufacturing and processing of glass it is necessary to predict the temperature for process design and control purposes. Since glass is a semitransparent (translucent) material at high temperatures, radiation can become an important or dominant heat transfer mechanism. Exact and approximate formulations for radiative transfer in glass are available [1 and 2]. Probably, the simplest approach is to consider radiation to be a diffusion process and to introduce the concept of the radiative conductivity which is analogous to the phonon thermal conductivity. However, serious questions have been raised about the validity of the approximation near interfaces and for glass of small spectral opacity.

The discrete ordinates method (DOM) has recently become popular and is commonly used for predicting radiative transfer in participating media [3], because it

is compatible with the finite-difference or finite-volume methods used in computational fluid mechanics and heat transfer. However, the DOM does not appear to have been applied to predict the temperature distribution and heat transfer in hot glass when the spectral absorption coefficient ranges over almost three orders of magnitude in the spectral region between 0.4 to 5.0  $\mu\text{m}$  [4].

The purpose of the present paper is to examine the DOM and the diffusion approximation for predicting radiation transfer in a layer of glass and particularly near interfaces. A simple one-dimensional physical situation is considered which allows for a very critical assessment of these two methods by comparing the temperature distributions and heat transfer results based on these two approaches with those based on the exact formulation of radiative transfer [1]. Clear float and green glass are taken as typical examples, and spectral absorption coefficients reported in the literature [4] are used in the calculations. The requirement to predict accurately the temperature distribution and heat transfer near the boundaries and the need to identify an accurate and computationally efficient method for radiative transfer have motivated the work reported in the paper.

---

Received 15 October 1997, revised manuscript 26 January 1999.

<sup>1)</sup> Presently at School of Mechanical Engineering, Pusan National University, Pusan (Korea).

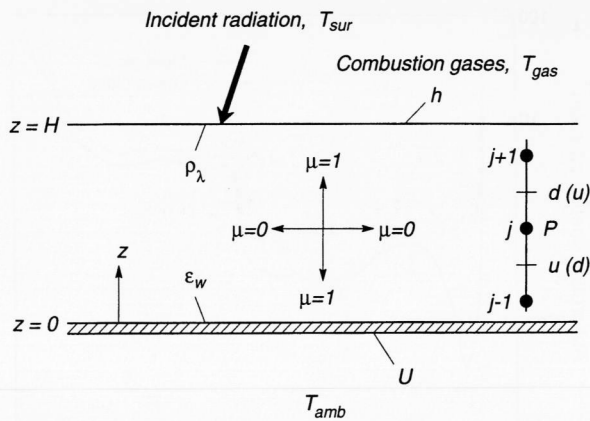


Figure 1. Schematic of the physical model and coordinate system.

## 2. Analysis

### 2.1 Model equation

Consider heat transfer within a plane layer of glass shown in figure 1. On the bottom the glass is in contact with an opaque material which is taken to be a diffuse reflector and emitter of radiation. The glass is heated from above with high-temperature combustion gases. This is intended to simulate the conditions in a glass melting furnace, refiner or forehearth [2]. It is assumed that the top surface of the glass is optically smooth and specularly reflecting. At the free surface the glass layer is heated by convection from hot combustion gases and by radiation from the gases and hot refractory surfaces. Heat transfer by convection is estimated by specifying the convective heat transfer coefficient  $h$ , and the refractive index of combustion gas is assumed to be unity. Heat transfer through the opaque boundary at the bottom is calculated by specifying the overall heat transfer coefficient  $U$ . Heat transfer within the glass layer is by combined conduction and radiation; advection is neglected. The glass is assumed to be a homogeneous, absorbing and emitting material, and scattering is neglected in comparison with absorption. In addition, the following assumptions are made in the analysis: a) the medium is at local thermodynamic equilibrium for which Planck's and Kirchhoff's laws are valid; b) the spatial dimensions of the medium are much larger than the wavelength of radiation for the semitransparent band, i.e., the coherence effects are negligible; c) the refractive index of the medium does not depend on the temperature in the considered range.

Under the physical situation considered, the one-dimensional energy equation in the glass layer is

$$\left. \begin{aligned} \frac{d}{dz} \left( -k \frac{dT}{dz} + F \right) &= 0 \\ \text{or} \\ -k \frac{dT}{dz} + F &= \text{constant} \end{aligned} \right\} \quad (1)$$

This equation states that the sum of the conductive ( $-k dT/dz$ ) and the radiative fluxes ( $F$ ) is constant at any horizontal plane in the layer. The divergence of the radiative flux is obtained by integrating the divergence of the spectral flux over the part of the spectrum in which the glass is considered to be semitransparent to radiation,

$$\frac{dF}{dz} = \int_0^{\lambda_{\text{cut}}} \frac{dF_{\lambda}}{dz} d\lambda = \int_0^{\lambda_{\text{cut}}} \kappa_{\lambda} \{4\pi n_{\lambda}^2 I_{b\lambda}[T(z)] - G_{\lambda}(z)\} d\lambda \quad (2)$$

where the cut-off wavelength  $\lambda_{\text{cut}}$  indicates the wavelength for which the medium is considered to be opaque to radiation. The spectral radiative flux  $F_{\lambda}$  and the spectral irradiance  $G_{\lambda}$  are defined as

$$F_{\lambda}(z) = 2\pi \int_{-1}^1 I_{\lambda}(z, \mu) \mu d\mu \quad (3)$$

and

$$G_{\lambda}(z) = 2\pi \int_{-1}^1 I_{\lambda}(z, \mu) d\mu \quad (4)$$

respectively. In these equations  $I_{\lambda}(z, \mu)$  denotes the spectral radiation intensity which is a function of the direction  $\mu$  ( $=\cos \theta$ ) at any position  $z$ . The divergence of the radiative flux defined in equation (2) is obtained by solving the radiative transfer equation (RTE) within the semitransparent (absorbing and emitting) medium [2].

To solve the energy equation (1), boundary conditions are required at each interface of the glass layer. These conditions are obtained from energy balances. The interface energy balance provides the following relation for the top surface of the layer,

$$\begin{aligned} -k \frac{dT}{dz} \Big|_{z=H} &= h[T(z=H) - T_g] \\ &+ \varepsilon_{\text{op}} \pi \left\{ \int_{\lambda_{\text{cut}}}^{\infty} I_{b\lambda}[T(z=H)] d\lambda - \int_{\lambda_{\text{cut}}}^{\infty} I_{b\lambda}(T_{\text{sur}}) d\lambda \right\} \end{aligned} \quad (5)$$

where  $\varepsilon_{\text{op}}$  is the emissivity for the spectral range where the glass is considered to be opaque to radiation.

At the bottom of the layer, the boundary condition can be expressed as

$$\begin{aligned} k \frac{dT}{dz} \Big|_{z=0} &= U[T(z=0) - T_{\text{amb}}] \\ &+ \varepsilon_w \left\{ \int_0^{\lambda_{\text{cut}}} \pi I_{b\lambda}[T(z=0)] d\lambda - \int_0^{\lambda_{\text{cut}}} F_{\lambda}^{-}(z=0) d\lambda \right\} \end{aligned} \quad (6)$$

where  $\varepsilon_w$  is the emittance of the opaque bottom, which is assumed to be diffuse and gray.

### 2.2 Radiative transfer model – discrete ordinates method

The radiative transfer equation (RTE) for a spectrally absorbing-emitting medium can be written as [2]

$$\mu \frac{dI_\lambda}{dz} = \kappa_\lambda \{n_\lambda^2 I_{b\lambda}[T(z)] - I_\lambda(z, \mu)\} \quad (7)$$

where  $I_\lambda(z, \mu)$  is the spectral intensity of radiation, which is a function of position, direction and wavelength, and  $I_{b\lambda}(T)$  is the spectral intensity of blackbody radiation given by Planck's function. The boundary condition for equation (7) at an optically smooth free surface from the interface conditions between the glass and the bounding entity is written as

$$I_\lambda(H, \mu) = [1 - \rho_\lambda(\mu)] n_\lambda^2 I_{b\lambda}(T_{sur}) + \rho_\lambda(\mu) I_\lambda(H, \mu') \quad (8)$$

The direction cosines  $\mu$  and  $\mu'$  are related through Snell's law. The interaction of radiation at the smooth interface between two dielectric media is governed by Fresnel's law [2]. The directional reflectivity,  $\rho_\lambda(\mu)$ , of the interface between two dielectric media of different refractive indices is obtained by combining Fresnel's equation for reflection and Snell's law for refraction,

$$\left. \begin{aligned} \rho_\lambda(\mu) &= 1 \\ \text{for } \mu < \mu_{crit}, \\ \rho_\lambda(\mu) &= \frac{1}{2} \left( \frac{\mu - n_\lambda P_\lambda}{\mu + n_\lambda P_\lambda} \right)^2 + \frac{1}{2} \left( \frac{n_\lambda \mu - P_\lambda}{n_\lambda \mu + P_\lambda} \right)^2 \\ \text{for } \mu \geq \mu_{crit} \end{aligned} \right\} \quad (9)$$

where  $P_\lambda = \sqrt{1 - n_\lambda^2(1 - \mu^2)}$  and  $\mu_{crit}$  is the critical angle given by Snell's law [3]. The boundary conditions at the opaque surface of the bottom is similarly written as

$$I_\lambda(0, \mu) = \epsilon_w n_\lambda^2 I_{b\lambda}[T(z=0)] + (1 - \epsilon_w) I_\lambda(0, \mu') \quad (10)$$

The radiative transfer equation, equation (7), for a spectrally emitting and absorbing medium along a specified discrete direction  $\mu^m$  can be expressed as

$$\mu^m \frac{dI_\lambda^m}{dz} = \kappa_\lambda \{n_\lambda^2 I_{b\lambda}[T(z)] - I_\lambda^m\} \quad (11)$$

This ordinary differential equation must be solved for every direction  $\mu^m$  to determine the spectral radiation field  $I_\lambda(z, \mu)$ .

The spatially discretized radiative transfer equation in terms of the radiative intensities on the control surface can be obtained by integrating over the control volume, and the final form of both directionally and spatially discretized algebraic equation is expressed as

$$I_{\lambda,P}^m = \frac{|\mu^m| I_{\lambda,u}^m / f_z + n_\lambda^2 \kappa_\lambda \Delta z I_{b\lambda,P}}{|\mu^m| / f_z + \kappa_\lambda \Delta z} \quad (12)$$

where

$$\Delta z = |z_u - z_d| \quad (13)$$

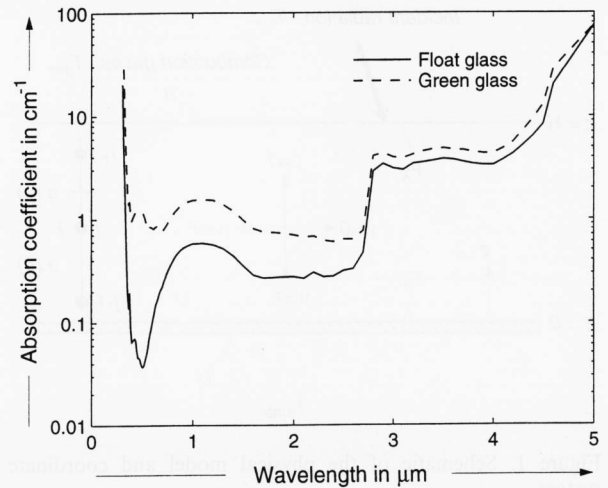


Figure 2. Spectral absorption coefficients for soda-lime float glasses.

Equation (12) is applicable to the case where  $\mu^m$  is either positive or negative.

A differencing scheme was introduced in order to reduce the number of the unknowns in equation (12). The spectral radiative intensity,  $I_{\lambda,P}^m$ , at the center of the control volume can be related to the intensities at the control surfaces ( $I_{\lambda,d}^m, I_{\lambda,u}^m$ ) by

$$I_{\lambda,P}^m = (1 - f_z) I_{\lambda,u}^m + f_z I_{\lambda,d}^m \quad (14)$$

The value of the weighting factor  $f_z$  must be restricted within the range of  $0 < f_z \leq 1$ . Taking  $f_z = 0.5$  yields the diamond or central differencing scheme proposed by Carlson and Lathrop [5], and taking  $f_z = 1$  yields the step or upwind differencing scheme. In addition, positive [6] and exponential [5] schemes are tested to check the sensitivity of the results to the differencing scheme.

### 2.3 Thermophysical and radiative properties of glass

The soda-lime glass is widely used and is taken as an example for the purpose of the present study. The thermal conductivity of the soda-lime glass is given by an empirical relation by Mann et al. [7].

The refractive indices and the absorption coefficients of the soda-lime glasses reported by Rubin [4] are used. Figure 2 shows the absorption coefficients for two types of glasses. The absorption coefficient  $\kappa_\lambda$  of clear float glass is relatively small in the visible and near infrared parts of the spectrum. Float glass has a good transmission in this spectral region. Green glass has relatively higher values of the absorption coefficient. Both glasses are considered to be opaque to radiation for wavelengths larger than the cut-off wavelength  $\lambda_{cut}$ , which is assumed to be  $5 \mu m$ . The emissivity in the opaque spectral region ( $\lambda \geq \lambda_{cut}$ ) is  $\epsilon_{op} = 0.9$ .

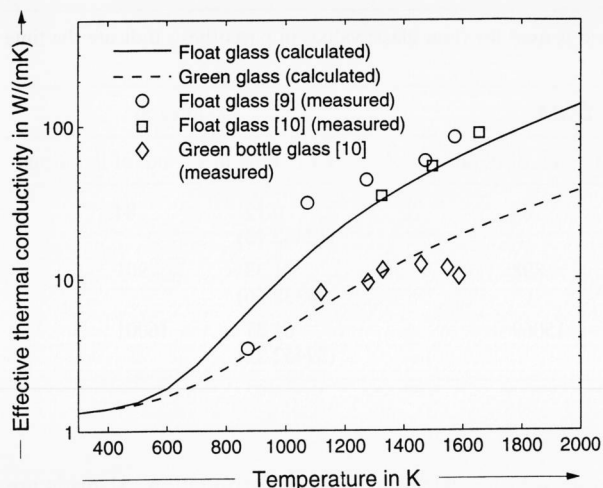


Figure 3. Effective thermal conductivity for soda-lime glasses.

#### 2.4 Radiative transfer model – diffusion approximation

Rigorous analysis of radiative transfer is rather complex and requires considerable computer resources. Thus, in order to simplify the analysis, a number of approximate approaches have been suggested [1, 8 to 10]. The Rosseland diffusion approximation is the simplest and the most commonly used approach. It has been known to glass scientists and technologists for a long time. Using this approximation, the radiative flux in a one-dimensional plane layer can be expressed as

$$F = -k_R \frac{dT}{dz} \quad (15)$$

where  $k_R$  is the radiative conductivity of the material defined as

$$k_R = \frac{4\pi}{3} \int_0^\infty \frac{n_\lambda^2}{\kappa_\lambda} \left( \frac{dI_{d\lambda}}{dT} \right) d\lambda \quad (16)$$

This conductivity is known as the Rosseland radiative conductivity. Even though the diffusion approximation is very simple it breaks down in the vicinity of the boundary and/or when the opacity of the material is not sufficiently large.

The effective thermal conductivity is the sum of the phonon thermal conductivity and Rosseland thermal conductivity given by equation (16). The spectral absorption coefficients reported by Rubin [4] are used to calculate  $k_R$ . Figure 3 shows a comparison of the calculated effective thermal conductivity and the measured data [9 and 10]. The effective thermal conductivities calculated for the float and green glasses are in good agreement with measured results and, therefore, are used in the present analysis.

#### 2.5 Method of solution

Since the energy equation is nonlinear when radiative transfer has been included, the solution is obtained numerically. The finite volume method is used to solve the thermal energy equation. Both the diffusion approximation and the discrete ordinates method are used to calculate the radiative transfer as described in subsections 2.4 and 2.2, respectively.

The accuracy of the discrete ordinates method depends on the choice of the quadrature set. Although the choice is arbitrary, a completely symmetric quadrature is preferred in order to preserve geometric invariance of the solution [11]. Moreover, the directional dependence of specularly reflecting boundaries is affected by the choice of the quadrature set to be used, because the weight represents a part of the area on a unit sphere for each ordinate direction, and the average value of reflectivity within the range of a weight varies with the type of the quadrature set. Thus, the dependence of reflectivity on quadrature sets was examined [12], and the level symmetric odd (LSO) quadrature was found to yield improved results for larger refractive index ( $n = 1.50$ ). In the present study, an average value of the refractive index over the whole spectrum is used ( $n = 1.49$ ), and the  $S_8$  LSO quadrature is adopted.

For a one-dimensional problem, the integral (exact) solution of the radiative transfer equation is available [1 and 13], but it requires much computer time to evaluate the exponential integral functions numerically and accurately. Since the integral functions include spectral radiative properties [1], the number of numerical integrations required greatly increases with the opacity of the medium. In order to obtain the results using the integral formulation [1 and 13], an accurate numerical integration scheme is needed. The ten-point Gaussian quadrature is used for the numerical integration by dividing the interval between the two nodes into ten uniform segments. The Gaussian quadrature is adopted for the small interval of each segment.

The grid spacing used is nonuniform and is more compact near the bounding interfaces. This was done in order to resolve the steep spatial changes in the physical variables expected in these regions. A sensitivity test for the grid size has been carried out, and a 51 nonuniform grid has been found to be enough to obtain accurate numerical results using the discrete ordinates method with the diamond scheme. Thus, the 51 nonuniform grid is preferably used. Otherwise, it will be mentioned.

The variation of the spectral absorption coefficient of the soda-lime glass with wavelength is not a smooth function and must be approximated. The most straightforward procedure is to use a band approximation. In a band model approach, a series of finite spectral intervals is used where the absorption coefficient is assumed to be constant at the average value in each interval. An eight spectral band model is used employing the data reported by Rubin [4].



Table 1. The computer time and the number of iterations when 51 grid is used for float glass; values in parenthesis indicate the time elapsed on an IBM workstation RS6000

$H$ in m	diffusion		DOM		integral	
	CPU time in s	no. of iterations	CPU time in s	no. of iterations	CPU time in s	no. of iterations
0.01	0.02 (17.97)	12	1.31 (143.73)	84	0.17 (12432.13)	84
0.1	0.03 (18.12)	17	14.75 (1521.88)	898	1.33 (8338.56)	901
1.0	0.17 (18.55)	102	454.25 (50998.97)	15069	61.37 (39452.22)	16001

The energy equation is solved iteratively until the relative error in temperature and radiative intensities between two sequential iterations is less than  $1 \cdot 10^{-8}$ . Thus, the constant total flux distribution over the glass layer as required by the energy equation (1) is obtained.

### 3. Results and discussion

#### 3.1 Description of physical model

There are a large number of model parameters, thermal conditions, etc., that describe the glass layer and its physical situation; therefore, it is necessary to be selective. The dimensions of the layer considered here and the temperature conditions are as follows:

thickness:	$H = 0.01, 0.1, 1.0$ m,
gas temperature:	$T_{\text{gas}} = 1800$ K,
surrounding temperature:	$T_{\text{sur}} = 1800$ K,
ambient temperature:	$T_{\text{amb}} = 300$ K,
convective heat transfer coefficient:	$h = 100$ W/(m <sup>2</sup> K),
overall heat transfer coefficient:	$U = 100$ W/(m <sup>2</sup> K).

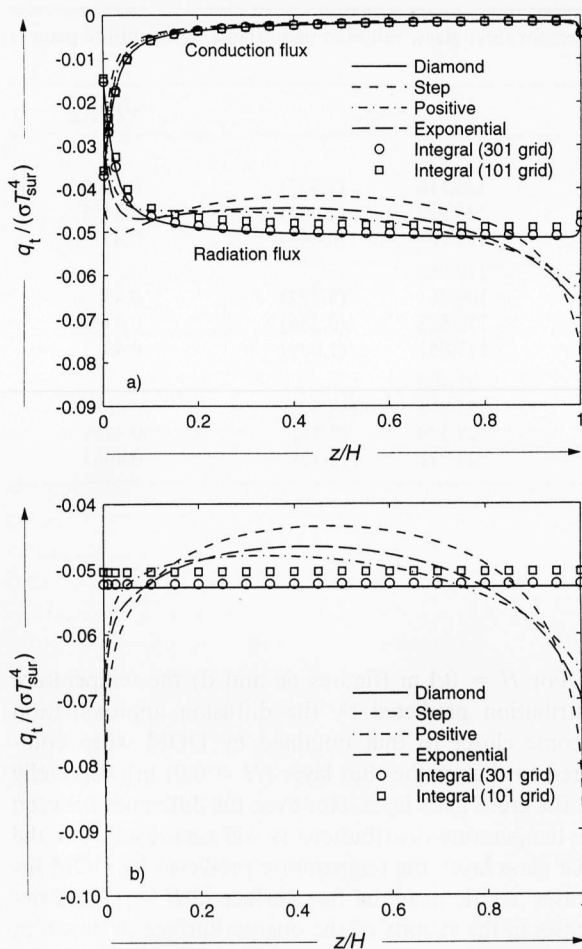
The surroundings are also assumed to be black and at the same temperature as combustion gas ( $T_{\text{sur}} = T_{\text{gas}}$ ). The spectral incident intensity is evaluated using Planck's function,  $I_{b\lambda}(T_{\text{sur}})$ . The emissivity of the opaque bounding wall may be chosen arbitrarily; but, the wall is assumed to be black for the sake of simplicity. The opaque boundary may be the surface of a thick wall, and the heat loss through it is expressed in terms of the overall heat transfer coefficient  $U$ . In glass melting systems this coefficient is a function of temperature and can be calculated from the knowledge of the refractories and their thicknesses.

#### 3.2 Model validation

Table 1 shows the computer time and the number of iterations required for a nonuniform grid of 51 nodes for float glass. For the diffusion approximation the computer time and the number of iterations are relatively small. For the exact integral equation formulation [1 and 13] for radiative transfer, they are relatively large due to the numerical integration. Moreover, to obtain the accu-

rate solution with the integral formulation, 51 grids are not sufficient, particularly when the layer thickness is small or large. As the layer thickness increases, the interval between the two integration limits also increases, and the numerical accuracy decreases. As the layer thickness decreases, the exponential integral function [3] varies sharply and a more accurate evaluation of integral is required. The results based on the integral formulation reported in the paper were obtained with a finer grid system, resulting in the increase of computer time greater than a factor of two or three. These results are not included in table 1. When the DOM is used, the computer time and the number of iterations are moderate for relatively thin ( $H = 0.01$  or  $0.1$  m) layers, but they are much larger for  $H = 1.0$  m.

The discrete ordinates method is used to solve the radiative transfer equation (7) and to calculate the radiative flux from equation (3). The flux obtained is used to solve the overall energy equation (1). As already mentioned, the energy equation (1) states that the total heat flux is constant at any plane in the layer. For the results obtained using the diffusion approximation, the total heat flux is constant over the layer regardless of the layer thickness and the grid size. However, the same is not always true for the results obtained using the discrete ordinates method. Figures 4a and b show heat flux distributions with various spatial differencing schemes. Only the total flux calculated with the diamond scheme is constant over the layer thickness as shown in figure 4b. This is due to false scattering which is artificially or numerically introduced by the spatial differencing schemes in the discrete ordinates method [14]. The conductive fluxes are nearly the same for the different schemes used as shown in figure 4a. Chai et al. [14] showed that the step scheme produces greatly smeared intensity fields by false scattering, whereas the diamond scheme produces less smearing. When the diamond scheme is used, however, some of the control surface intensities are negative and this is physically unrealistic. Thus, in general, to prevent the intensities from being negative, the resulting negative intensities are set to zero by the negative intensity modification ("fix-up") procedure [5]. The control surface intensities are set to zero to reduce the extent of false scattering. Regarding the



Figures 4a and b. Heat flux distributions with differencing schemes for float glass with  $H = 1.0$  m and 51 grid; a) conductive and radiative heat fluxes, b) total heat fluxes.

term “false scattering”, Jessee and Fiveland [15] have suggested and used the term “numerical smearing” instead of the former. From now on the phrase numerical smearing is employed in the paper.

Figures 4a and b reveal that the total fluxes obtained with the step scheme are highly nonuniform. The weighting factors of the positive or exponential schemes have values between 0.5 and 1.0, i.e., between the weighting factors of the diamond and step schemes. Thus, these two schemes also induce the numerical smearing and produce the nonuniform total flux distributions.

Table 2 shows that the total heat fluxes calculated with the diamond scheme are constant to within six or seven digits, but the fluxes with other schemes are constant only to within two or three digits even though the grid used is fine. Of the spatial differencing schemes except for the diamond scheme, the relative error for the positive scheme is the least and the relative error for the step scheme is the largest. With regard to the uniformity of total heat flux, the positive scheme is acceptable for  $H = 0.01$  m, but the accuracy is not sufficient for the thick layers. For  $H = 1.0$  m, only the diamond scheme exhibits a good total heat flux uniformity.

When the spatial differencing scheme is used, grid refinement results in an improved uniformity of the total heat flux distributions as shown. An example for  $H = 1.0$  m is illustrated in figure 5. The positive scheme with a grid larger than 401 nodes exhibits an acceptable uniformity of the total heat flux, but for the exponential scheme a grid larger than 501 nodes is needed. However, for the thick layer ( $H = 1.0$  m), the uniformity of total heat flux can not be obtained even with 501 grid and the positive scheme. If the opacity of the layer increases (i.e., as would for a green glass), a much greater number of nodes is required to obtain a constant total heat flux with the positive or exponential schemes. Therefore, even though the uniformity obtained by the positive scheme is gradually improved as the grid size increases, figure 5 shows that the diamond scheme is the best choice to obtain the constant total heat flux distributions.

In order to obtain the constant total flux distribution, the diamond scheme is used to obtain the results reported in this paper. However, the negative intensities caused by the diamond scheme at some control surfaces cause another problem. If the negative intensities are eliminated or not amplified during the iteration, converged solutions are obtained. Otherwise, the calculation scheme diverges. Even though converged results are obtained, the solutions can be distorted due to the oscillations caused by the undershoots (negative intensities) and the overshoots (intensities higher than the incident intensity) [16]. This is also unrealistic. In the present study, the distorted solutions do not appear. However, as indicated by Chai et al. [16], the fine grid can not be used, particularly for thick layers, because the negative intensities cause the iteration scheme to diverge. When  $H = 1.0$  m, a grid larger than 51 nodes causes the calculations to diverge.

### 3.3 Temperature distributions

The temperature distributions calculated using the diffusion approximation, the discrete ordinates method and rigorous integral equation formulation for radiative transfer are shown in figures 6 to 8<sup>2)</sup>. The temperature distributions predicted by DOM and the integral formulation are nearly identical and are not distinguishable from each other in the figures shown in the paper. Figures 6a to f show that the difference between the temperature distributions obtained with the diffusion approximation and the discrete ordinates method is large. The difference is primarily due to the fact that the long-range energy transport by radiation cannot be predicted by the diffusion approximation, particularly when the opacity of the glass layer is small. It is well-known that the predictions of the diffusion approxi-

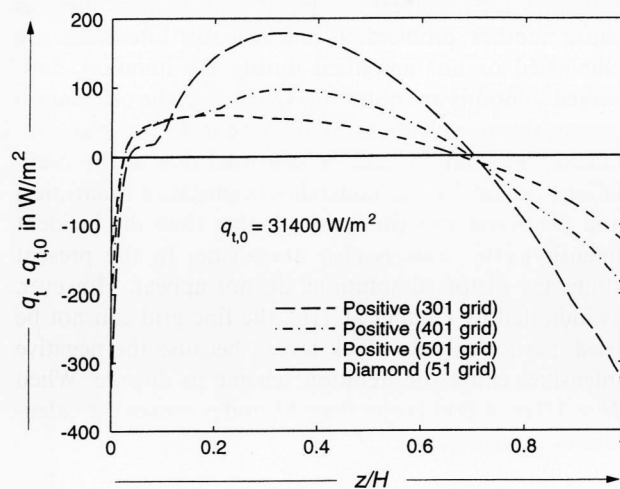
<sup>2)</sup> Note that in figures 6 through 8 the temperature distributions obtained using DOM fall practically on top of those based on the integral (exact) formulation, and separate curves could not be clearly indicated in the figures.

Table 2. Uniformity of total heat flux in kW/m<sup>2</sup> with differencing schemes for float glass; values in parenthesis represent the percent errors relative to the flux obtained with the diamond scheme

$H$ in m	differencing schemes	$(-q_t)_{\max}^3$		$(-q_t)_{\min}^4$		$z/H _{\min}$
0.01	diamond	135.989		135.989		
	step	136.029	(0.029)	134.116	(1.377)	0.5000
	positive	135.990	(0.001)	135.983	(0.004)	0.3455
	exponential	135.991	(0.002)	135.933	(0.041)	0.4373
0.1	diamond	119.088		119.088		
	step	120.659	(1.319)	109.261	(8.252)	0.4686
	positive	119.164	(0.064)	118.628	(0.386)	0.4373
	exponential	119.280	(0.161)	117.851	(1.039)	0.4373
1.0	diamond	31.400		31.400		
	step	53.662	(70.90)	25.873	(17.60)	0.4686
	positive	39.389	(25.44)	28.539	(9.11)	0.3159
	exponential	42.131	(34.18)	27.721	(11.72)	0.4063

<sup>3)</sup>  $(-q_t)_{\max}$  occurs at  $z/H = 0$  or  $1$ .

<sup>4)</sup>  $(-q_t)_{\min}$  occurs at  $z/H|_{\min}$ .

Figure 5. Heat flux distributions with grid size for  $H = 1.0$  m.

mation become closer to the exact solutions as the opacity of the medium increases [1]. The difference is larger for the float glass than for the green glass.

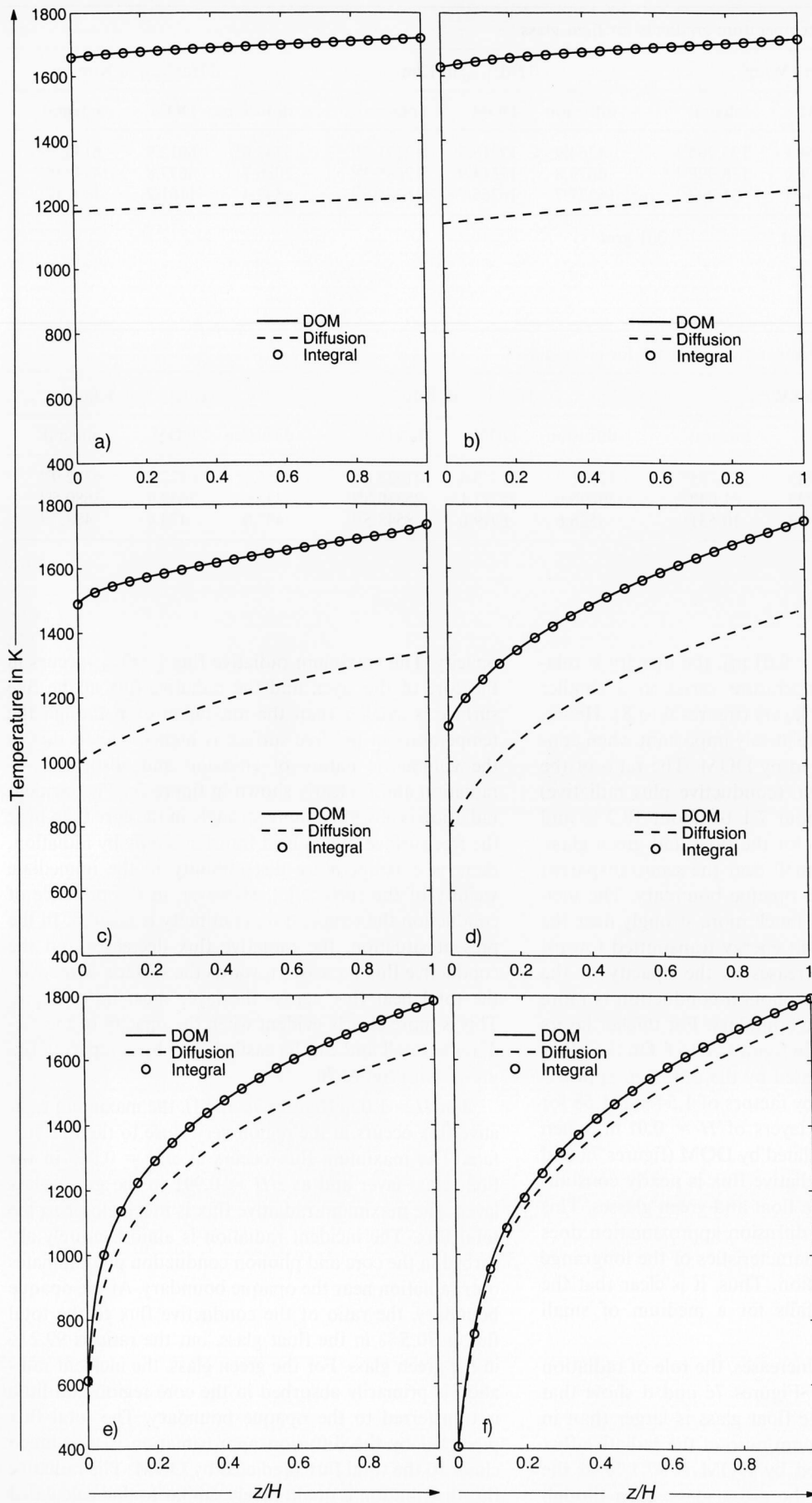
The temperature distributions predicted by the diffusion approximation for the two glasses are nearly linear (figures 6a and b). Since the layer thickness is small and the temperature range is small (i.e., about 1181 to about 1221 K for float glass and about 1140 to about 1248 K for green glass), the effective conductivities can be assumed to be constant. The temperature gradient is smaller for float glass than for green glass, because the effective conductivity is large, and thus the thermal resistance to heat conduction is small compared to the green glass. Accordingly, the heat flux is larger for the float glass compared to the green glass (see tables 3 and 4), and this is due to the larger effective conductivity of float glass.

For  $H = 0.1$  m (figures 6c and d) the temperature distribution predicted by the diffusion approximation become closer to that obtained by DOM when compared to that of the thin layer ( $H = 0.01$  m), especially for the green glass layer. However, the difference between the temperature distributions is still significant. For the float glass layer, the temperature predicted by DOM increases a little near the free surface ( $z/H = 1$ ) and decreases in the vicinity of the opaque surface as shown in figures 6c and d. Thus, the temperature gradients at the surfaces greatly differ from those obtained by the diffusion approximation (table 3). For the green glass layer (table 4), the difference between the temperature distributions decreases, especially near the opaque surface, and the gradients are closer to each other than for the float glass.

For  $H = 1.0$  m, the temperature distributions predicted by the diffusion approximation become much closer to those predicted by DOM as shown in figures 6e and f. The difference between the temperature distributions predicted by the two methods still exists, but it is much smaller in comparison to the thinner layers. For the green glass, the temperature differences at  $z = 0$  and  $z = H = 1.0$  m are 5.0 K and 61.5 K, respectively. The difference between the temperature gradients at each surface for the float glass layer is a little larger, but for the green glass layer the gradients are nearly the same, and the errors are within 10% as shown in table 4.

### 3.4 Heat transfer

Figures 7a to f show the heat flux distributions. The role of conduction and radiation for heat transfer across the glass layer is clearly shown in these figures. As the layer thickness increases, the opacity of the layer increases and radiative transfer plays a much more important role in the transfer of heat.



Figures 6a to f. Temperature distributions for: a)  $H = 0.01$  m, float glass; b)  $H = 0.01$  m, green glass; c)  $H = 0.1$  m, float glass; d)  $H = 0.1$  m, green glass; e)  $H = 1.0$  m, float glass; f)  $H = 1.0$  m, green glass.



Table 3. Total heat flux and temperature gradients for float glass

<i>H</i> in m	$-q_t$ in kW/m <sup>2</sup>			$dT/dz _{z=0}$ in K/m			$dT/dz _{z=H}$ in K/m		
	diffusion	DOM	integral	diffusion	DOM	integral	diffusion	DOM	integral
0.01	88.098	135.989	135.904 <sup>5)</sup>	4264.9	12310.5	12171.4 <sup>5)</sup>	3742.6	6012.9	6135.5 <sup>5)</sup>
0.1	70.184	119.088	118.998 <sup>6)</sup>	6679.8	12614.9	12685.2 <sup>6)</sup>	2086.7	4677.8	4748.9 <sup>6)</sup>
1.0	24.190	31.400	31.093 <sup>7)</sup>	16227.7	16365.7	16265.5 <sup>7)</sup>	349.4	1161.2	1197.6 <sup>7)</sup>

<sup>5)</sup> 101 grid.<sup>6)</sup> 201 grid.<sup>7)</sup> 301 grid.

Table 4. Total heat flux and temperature gradients for green glass

<i>H</i> in m	$-q_t$ in kW/m <sup>2</sup>			$dT/dz _{z=0}$ in K/m			$dT/dz _{z=H}$ in K/m		
	diffusion	DOM	integral	diffusion	DOM	integral	diffusion	DOM	integral
0.01	84.006	132.849	132.785 <sup>5)</sup>	12571.4	21478.4	21522.6 <sup>5)</sup>	9456.3	6322.2	6382.9 <sup>5)</sup>
0.1	49.654	81.223	81.042 <sup>6)</sup>	20696.6	25273.1	25330.8 <sup>6)</sup>	3333.6	3632.4	3680.5 <sup>6)</sup>
1.0	10.505	11.093	10.531 <sup>7)</sup>	8526.6	8979.6	8548.5 <sup>7)</sup>	437.0	473.4	488.7 <sup>7)</sup>

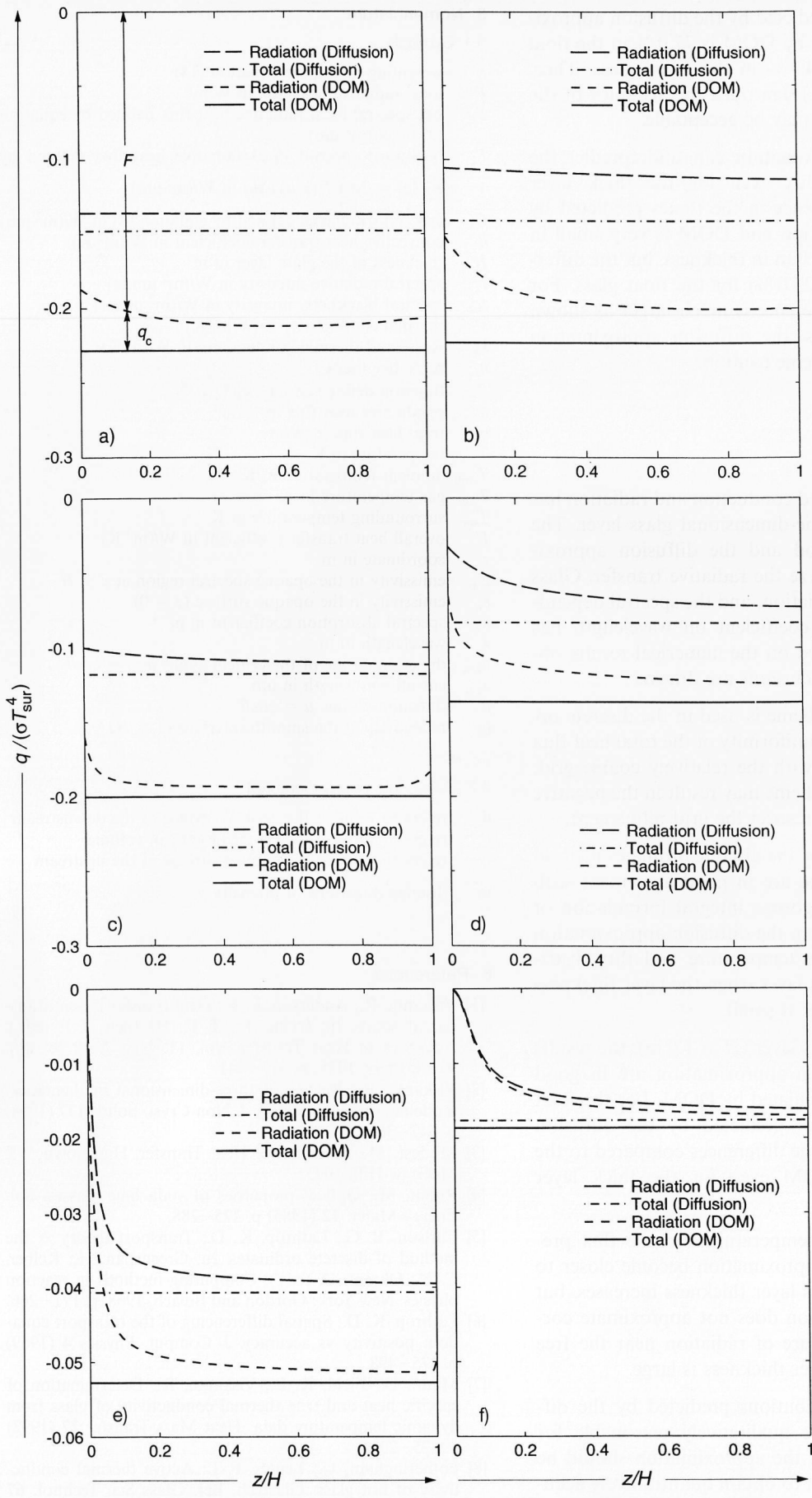
<sup>5)6)7)</sup> See table 3.

For the thin layer ( $H = 0.01$  m), the opacity is relatively small, and the temperature varies in a smaller range than for the thicker layers (figures 6 to 8). Hence, the conductive transfer is relatively important when considering the results obtained by DOM. The ratio of the conductive flux to the total (conductive plus radiative) flux is in the range of about 7.1 to about 18.2% and about 9.7 to about 32.1% for the float and green glass, respectively. The ratio is small near the semitransparent surface and large near the opaque boundary. The incident radiation is absorbed much more strongly near the free surface, and the radiant energy transmitted toward the opaque boundary decreases as the opacity of the glass layer increases. Thus, phonon conduction is more important near the opaque boundary. For thicker layers this trend is clearly shown in figures 7c to f. On the other hand, the total flux calculated by the diffusion approximation is underestimated by factors of 1.54 and 1.58 for the float and green glass layers of  $H = 0.01$  m, when compared to the flux calculated by DOM (figures 7a and b, tables 3 and 4). The radiative flux is nearly constant over the entire layer for the float and green glasses. This is due to the fact that the diffusion approximation does not properly resolve the characteristics of the longrange energy transport by radiation. Thus, it is clear that the diffusion approximation fails for a medium of small opacity.

As the layer thickness increases, the role of radiation becomes more important. Figures 7c and d show that the role of radiation in the float glass is larger than in the green glass. The maximum ratio of the radiative flux to the total flux calculated by DOM is 97.1% in the float glass and 90.8% in the green glass, even though the total flux is smaller in the green glass due to the large

opacity. The maximum radiative flux ( $-F_{\max}$ ) occurs in the core of the layer, and the radiative flux at the free surface is smaller than the maximum even though the temperature at the free surface is higher. This is due to the volumetric nature of emission and absorption of radiation and is clearly shown in figure 7c. The incident radiation is absorbed more strongly in the core than near the free surface. When heat transfer is only by radiation, there is a temperature discontinuity in the immediate vicinity of the surface [3]. However, in the presence of conduction the temperature continuity is insured. In the present situation, the radiative flux decreases and the conductive flux increases towards the surface. Moreover, the total heat flux across the layer must be constant. This is more clearly evident when the opacity of the medium is small and can be easily noted by comparing figure 7c with figure 7d.

For  $H = 1.0$  m (figures 7e and f), the maximum radiative flux occurs in the region very close to the free surface. The maximum flux occurs at  $z/H = 0.965$  in the float glass layer and at  $z/H = 0.991$  in the green glass layer. The maximum radiative flux is much closer to the total flux. The incident radiation is almost entirely absorbed in the core and phonon conduction predominates over radiation near the opaque boundary. At the opaque boundary, the ratio of the conductive flux to the total flux is 70.5% in the float glass, but the ratio is 99.2% in the green glass. For the green glass, the incident radiation is primarily absorbed in the core region and little is transferred to the opaque boundary. The total flux predicted by the diffusion approximation is also much closer to the total flux predicted by DOM. The radiative flux distribution is qualitatively similar to that calculated by DOM except for the region near the free surface. The



Figures 7a to f. Heat flux distributions for: a)  $H = 0.01$  m, float glass; b)  $H = 0.01$  m, green glass; c)  $H = 0.1$  m, float glass; d)  $H = 0.1$  m, green glass; e)  $H = 1.0$  m, float glass; f)  $H = 1.0$  m, green glass.

ratio of the total flux predicted by the diffusion approximation to that predicted by DOM is 77.0% in the float glass and approaches 94.7% in the green glass. Thus, for the green glass layer 1.0 m thick the accuracy of the diffusion approximation may be acceptable.

The diffusion approximation can underpredict the temperature and the flux even for the thick layer ( $H = 1.0$  m). The difference in the fluxes predicted by the diffusion approximation and DOM is very small in the green glass layer of 1.0 m in thickness, but the difference is relatively large (23.0%) for the float glass. For the thinner layer the difference is much larger as shown in tables 3 and 4. Thus, the diffusion approximation should be used with extreme caution.

#### 4. Conclusions

Heat transfer by combined conduction and radiation has been investigated in a one-dimensional glass layer. The discrete ordinates method and the diffusion approximation are used to analyze the radiative transfer. Glass is semitransparent to radiation, and the spectral dependence of the absorption coefficient on wavelength has been accounted for. Based on the numerical results obtained, the following conclusions are drawn:

- When the diamond scheme is used in the discrete ordinates method, the best uniformity of the total heat flux could be obtained even with the relatively coarse grid. However, the diamond scheme may result in the negative intensities and thus may restrict the grid refinement.
- The results predicted by the discrete ordinates method with the diamond scheme are in good agreement with those obtained by the rigorous integral formulation of radiative transfer. However, the diffusion approximation greatly underpredicts the temperature and flux distributions through the glass layer when the layer thickness or the opacity of the layer is small.
- Only for the green glass layer ( $H = 1.0$  m), the results predicted by the diffusion approximation are in good agreement with those calculated by DOM. For the float glass, the total heat flux predicted by the diffusion approximation reveals large differences compared to the fluxes calculated by DOM even for the thick layer ( $H = 1.0$  m).
- The behavior of the temperature and the flux predicted by the diffusion approximation become closer to that by DOM as the glass layer thickness increases, but the diffusion approximation does not approximate correctly the long-range nature of radiation near the free surface even when the layer thickness is large.
- The temperature distributions predicted by the diffusion approximation are qualitatively reasonable for optically thick layers, but the approximation should be used with extreme caution to obtain quantitatively accurate heat transfer predictions near the interfaces.

#### 5. Nomenclature

##### 5.1 Symbols

$f_z$	weighting factor, see equation (14)
$F$	local radiative heat flux in $\text{W}/\text{m}^2$
$F_\lambda$	net spectral local radiative heat flux defined by equation (3) in $\text{W}/(\text{m}^2 \mu\text{m})$
$F_\lambda^-$	backward spectral local radiative heat flux defined by $F_\lambda^-(z) = 2\pi \int_0^1 I_\lambda(z, \mu) \mu d\mu$ in $\text{W}/(\text{m}^2 \mu\text{m})$
$G_\lambda$	spectral irradiance defined by equation (4) in $\text{W}/(\text{m}^2 \mu\text{m})$
$h$	convective heat transfer coefficient in $\text{W}/(\text{m}^2 \text{K})$
$H$	thickness of the glass layer in m
$I_\lambda$	spectral radiative intensity in $\text{W}/(\text{m}^2 \mu\text{m sr})$
$I_{b\lambda}$	spectral blackbody intensity in $\text{W}/(\text{m}^2 \mu\text{m sr})$
$k$	thermal conductivity in $\text{W}/(\text{m K})$
$k_R$	Rosseland thermal conductivity in $\text{W}/(\text{m K})$
$n_\lambda$	refractive index
$P_\lambda$	function defined as $\sqrt{1 - n_\lambda^2(1 - \mu)^2}$
$q_c$	conductive heat flux in $\text{W}/\text{m}^2$
$q_t$	total heat flux in $\text{W}/\text{m}^2$
$T$	temperature in K
$T_{\text{amb}}$	ambient temperature in K
$T_{\text{gas}}$	gas temperature in K
$T_{\text{sur}}$	surrounding temperature in K
$U$	overall heat transfer coefficient in $\text{W}/(\text{m}^2 \text{K})$
$z$	coordinate in m
$\epsilon_{\text{op}}$	emissivity in the opaque spectral region at $z = H$
$\epsilon_w$	emissivity in the opaque surface ( $z = 0$ )
$\kappa_\lambda$	spectral absorption coefficient in $\text{m}^{-1}$
$\lambda$	wavelength in m
$\mu_{\text{crit}}$	direction cosine of the critical angle, $\mu_{\text{crit}} = \cos\theta_{\text{crit}}$
$\lambda_{\text{cut}}$	cut-off wavelength in $\mu\text{m}$
$\mu$	direction cosine, $\mu = \cos\theta$
$\rho_\lambda$	reflectivity at the smooth interface ( $z = H$ )

##### 5.2 Subscripts and superscript

d	refers to value at the control surface of the downstream
P	refers to value at the center of control volume
u	refers to value at the control surface of the upstream
m	discrete directions of intensity

#### 6. References

- Viskanta, R.; Anderson, E. E.: Heat transfer in semitransparent solids. In: Irvine, Jr., T. F.; Hartnett, J. P. (eds.): *Advances in Heat Transfer*. Vol. 11. New York (et al.): Acad. Press, 1975. p. 317–441.
- Viskanta, R.: Review of three-dimensional mathematical modeling of glass melting. *J. Non-Cryst. Solids* **177** (1994) p. 347–362.
- Modest, M. F.: *Radiative Heat Transfer*. Highstown, NJ: McGraw-Hill, 1993.
- Rubin, M.: Optical properties of soda lime glasses. *Sol. Energy Mater.* **12** (1985) p. 275–288.
- Carlson, B. G.; Lathrop, K. D.: Transport theory – the method of discrete ordinates. In: Greenspan, H.; Kelber, C. N.; Okrent, D. (eds.): *Computing methods in reaction physics*. New York: Gordon and Breach, 1968. p. 171–266.
- Lathrop, K. D.: Spatial differencing of the transport equation: positivity vs accuracy. *J. Comput. Physics* **4** (1969) p. 475–498.
- Mann, D.; Field, R. E.; Viskanta, R.: Determination of specific heat and true thermal conductivity of glass from dynamic temperature data. *Heat Mass Transfer* **27** (1992) p. 225–231.
- Fotheringham, U.; Lentz, F.-T.: Active thermal conductivity of hot glass. *Glastech. Ber. Glass Sci. Technol.* **67** (1994) no. 12, p. 335–342.

- [9] Blažek, A.; Endrýs, J.; Kada, J.: Strahlungwärmeleitfähigkeit von Glas – Einfluß der Glaszusammensetzung auf seine Wärmedurchlässigkeit. *Glastechn. Ber.* **49** (1976) no. 4, p. 75–81.
- [10] Endrýs, J.; Blažek, A.; Ederová, J.: Experimental determination of the effective thermal conductivity of glass by steady-state method. *Glastech. Ber.* **66** (1993) nos. 6/7, p. 151–157.
- [11] Lathrop, K. D.; Carlson, B. G.: Discrete ordinates angular quadrature of neutron transport equation. Technical report LA-3186. Los Alamos, NM: Los Alamos Scientific Laboratory, 1965.
- [12] Lee, K. H.; Viskanta, R.: Prediction of spectral radiative transfer in a condensed cylindrical medium using discrete ordinates method. *J. Quant. Spectrosc. Radiat. Transfer* **33** (1997) p. 5–22.
- [13] Viskanta, R.; Song, T.-H.: On the diffusion approximation for radiation transfer in glass. *Glastech. Ber.* **58** (1985) no. 4, p. 80–86.
- [14] Chai, J. C.; Lee, H. S.; Patankar, S. V.: Ray effect and false scattering in the discrete ordinates method. *Numer. Heat Transfer Pt.B.* **24** (1993) p. 373–389.
- [15] Jessee, J. P.; Fiveland, W. A.: Bounded, high-resolution differencing schemes applied to the discrete ordinates method. *J. Thermophys. Heat Transfer* **11** (1997) no. 4, p. 540–548.
- [16] Chai, J. C.; Patankar, S. V.; Lee, H. S.: Evaluation of spatial differencing practices for the discrete-ordinates method. *J. Thermophys. Heat Transfer* **8** (1994) p. 140–144.

■ 0899P002

Addresses of the authors:

R. Viskanta  
Purdue University  
Heat Transfer Laboratory  
1288 School of Mechanical Engineering  
West Lafayette, IN 47907-1288 (USA)

K. H. Lee  
Pusan National University  
School of Mechanical Engineering  
San 30, Jangjeon-Dong, Kumjung-Ku  
Pusan 609-735 (Korea)